DOI: 10.4408/IJEGE.2017-01.S-04

COUPLING 3D HYDROGEOLOGICAL MODELLING AND GEOCHEMICAL MAPPING FOR AN INNOVATIVE APPROACH TO SUPPORT MANAGEMENT OF AQUIFERS

Stefania DA PELO(*), Giorgio GHIGLIERI(**), Cristina BUTTAU(***), Riccardo BIDDAU(*), Claudio CUZZOCREA(***), Antonio FUNEDDA(*), Alberto CARLETTI(**), Salvatore VACCA(*) & Rosa CIDU(*)

(*) University of Cagliari - Department of Chemical and Geological Sciences - Via Trentino, 51 - 09127 Cagliari, Italy
(**) University of Cagliari - Department of Chemical and Geological Sciences - Via Trentino, 51 - 09127 Cagliari, Italy and University of Sassari - Desertification Research Center - NRD - Viale Italia, 39 - 07100 Sassari, Italy
(***) University of Sassari - Desertification Research Center - NRD - Viale Italia, 39 - 07100 Sassari, Italy
Corresponding author: sdapelo@unica.it

EXTENDED ABSTRACT

Nell'ambito del progetto KNOW (implementing the Knowledge of NitrOgen in groundWater), uno dei progetti di ricerca finanziati dalla Regione Sardegna per le finalità previste dalla Legge Regionale n. 7 del 2007, è stato condotto uno studio con l'obiettivo di migliorare le conoscenze di base sulle metodologie per la comprensione ed il monitoraggio delle dinamiche di trasferimento degli inquinanti nelle acque sotterranee. Obiettivo specifico è stato quello di fornire dei sistemi innovativi ed integrati per la definizione dei processi di degrado delle risorse idriche sotterranee.

In questo lavoro viene presentata una proposta metodologica per la ricostruzione e la definizione delle caratteristiche idrogeologiche di acquiferi complessi. La metodologia è stata applicata al bacino pilota della Nurra, nella Sardegna nord-occidentale. In tale settore sono stati condotti numerosi studi, tuttavia la complessità geologica e la varietà delle litologie presenti rende problematica la ricostruzione della circolazione idrica e delle geometrie dei corpi idrici sotterranei. Sulla base di studi precedenti è stato stabilito che le riserve idriche sotterranee sono ospitate principalmente nelle coperture carbonatiche mesozoiche. Esse sono rappresentate, dal basso verso l'alto, da tre unità idrogeologiche principali: l'acquifero del Trias, costituito da dolomie e calcari, con importanti livelli evaporitici (essenzialmente gessi); l'acquifero del Giurassico, il più importante, con uno spessore di oltre 700 m, costituito da dolomie e calcari con intercalazioni marnose; l'acquifero del Cretaceo, costituito da calcari e marne. Sulle successioni carbonatiche mesozoiche poggiano flussi piroclastici, spesso alterati in argille smectitiche e coperture alluvionali neogeniche. La successione mesozoica è caratterizzata dalla sovrapposizione di due sistemi di pieghe che conferiscono all'area una caratteristica geometria a duomi e bacini. Il primo sistema ha interessato la piattaforma carbonatica mesozoica durante il Cretaceo medio dando luogo a sovrascorrimenti orientati NW-SE immergenti verso NE e ad ampie pieghe con piani assiali subverticali o immergenti verso NE ed assi orientati NW-SE. Il secondo sistema ha coinvolto anche i depositi del Cretaceo superiore, ma non la successione vulcano-sedimentaria terziaria, e ha dato luogo a un sistema di pieghe orientate NE-SW.

Allo scopo di definire le geometrie e le relazioni fra i diversi acquiferi, è stato ricostruito un modello idrogeologico 3D. L'elaborazione del modello è stata eseguita a partire da sezioni geologico-strutturali opportunamente orientate e bilanciate, basate sulla cartografia geologica del progetto CARG (in scala 1:50.000), sulla cartografia della Regione Sardegna (in scala 1:25.000) e su quella elaborata nell'ambito del progetto RIADE (in scala 1:50.000). Inoltre, i log stratigrafici di sondaggi e pozzi provenienti da archivi regionali e da studi precedenti hanno permesso di ottenere un maggiore dettaglio nella proiezione in profondità dei dati cartografici. Data la variabilità delle fonti da cui si è attinto, è stato necessario operare un processo di validazione, omogenizzazione e standardizzazione dei dati. Una volta verificati, i dati sono stati implementati nel modello mediante la creazione di un geodatabase, digitalizzati in ambiente GIS ed elaborati nell'ambiente 3D con il software Midland Valley's 3D MOVE. L'elaborazione del modello geologico-strutturale 3D è stato quindi integrato con informazioni di tipo idrogeologico e geochimico, anch'esse implementate nel modello attraverso il geodatabase. La ricostruzione 3D idrogeologica, insieme alla cartografia geochimica e all'utilizzo di tecniche statistiche multivariate (analisi delle componenti principali) hanno permesso di dimostrare che il campo di moto dell'acquifero è fortemente influenzato dai sistemi di pieghe, faglie dirette e sovrascorrimenti individuati nell'area. In particolare, nell'acquifero del Giurassico, essi producono direzioni di drenaggio principali verso NE nel settore nord e verso SW nel settore sud. I sovrascorrimenti a basso angolo con direzione NW mettono in contatto l'acquifero del Giurassico con quello del Trias nel settore più occidentale della regione, come anche messo in evidenza attraverso l'analisi geochimica. L'approccio utilizzato in questo studio ha dimostrato come l'integrazione di strumenti geochimici all'interno del quadro fisico di un modello geologico può essere utile a meglio comprendere e concettualizzare i sistemi idrogeologici in contesti geologici complessi. Tali informazioni sono un imprescindibile prerequisito per la valutazione della potenziale dispersione degli inquinanti nelle acque sotterranee e per la gestione delle risorse idriche.

ABSTRACT

A methodological approach to assess the hydrogeological feature in complex hydrogeological situations is proposed. It provided a hydrogeological 3D modelling, supported by hydrogeochemical mapping and integrated interpretation of available data. The proposed methodology was applied to the strategic aquifer of the Nurra district (NW Sardinia, Italy). The finding of this work highlighted that structural history of the Nurra district exerts a relevant control on the hydrogeology and hydrochemistry of groundwater. The local connection of Triassic and Jurassic aquifers was proposed. The knowledge-base system will provide a suitable and effective tool for understanding and monitoring the dynamics of pollutant transfer into groundwater to better manage water resources and mitigate desertification processes.

***Keywords**: 3D hydrogeological model, hydrogeochemistry, pollution, desertification, Sardinia, Italy*

INTRODUCTION

The concern about the potential pollution of groundwater because of increasing human pressure on the environment has led to the development of an extensive legal framework. Both the 91/676/EEC and 2006/118/EC Directives concerning respectively "the protection of waters from nitrate of agricultural sources", and "the protection of groundwater against pollution and deterioration (GroundWater Directive, GWD)", have been implemented in Italy.

The Nurra district (NW Sardinia, Italy) has been affected by several detrimental effects on groundwater due to intense human activities and recent climatic changes, which made this area vulnerable to desertification (Ghiglieri *et alii*, 2009a), threatened by salinization processes (Ghiglieri *et alii*, 2012; Mongelli *et alii*, 2013) and subjected to nitrate contamination (Ghiglieri *et alii*, 2009b; ARPAS, 2009; RAS, 2014). Water supplies in the Nurra district are secured largely by surface waters impounded in reservoirs. However, groundwater is exploited using boreholes, including five wells discharging a total of 96 L/s to satisfy water demand of the city of Alghero, where population increases from almost 53,000 to 110,000 inhabitants in the summer (RAS, 2006a; Ghiglieri *et alii*, 2009a). Therefore, groundwater represents a strategic and essential alternative resource, especially given the increased demand of water for human consumption, agriculture and the extreme droughts and floods that have affected this region over the last 15 years. Previous investigations found that deep geological structures control groundwater circulation (Ghiglieri *et alii*, 2006; 2009a; 2014). However, reconstruction of the geometry of the aquifers, groundwater flow and the related quality was made difficult by the geological complexity.

The present study has been carried out within the framework of the KNOW project (implementing Knowledge of NitrOgen in groundWater) funded under the Regional Law 7/2007 by the Regional Government of Sardinia (Da Pelo *et alii*, 2015). Aim of the project was improving a knowledge-base system for understanding and monitoring transfer dynamics of pollutants into groundwater, especially those related to agricultural practice. In order to achieve properly the objectives of the research, it was considered necessary to apply an interdisciplinary approach, addressed to integrate structural-geological, stratigraphic, hydrogeological and geochemical data using a Geographical Information System (GIS).

Main objective of this study was to apply innovative technologies to develop a 3D geological - structural model of the Nurra district integrating it with hydrogeological and geochemical information, in order to reconstruct the geometry and the relationship among the aquifers (Chesnaux *et alii*, 2011; Zhu *et alii*, 2012; Ghiglieri *et alii*, 2016). Such information is a needful prerequisite to evaluate the dispersion of pollutants in groundwater (Raiber *et alii*, 2012). Spatial distributions of chemical elements presented as geochemical maps allow a better visualization of the geochemical processes active in a study area, thus facilitating the decision-making process in water resources management and assessment (Ohta *et alii*, 2015; Lancianese & Dinelli, 2015).

STUDY AREA

The Nurra district consists of a structural high tilted to the east, which developed during Tertiary (Ghiglieri *et alii*, 2009a; Mongelli *et alii*, 2013), whose eastern limit is marked by the Upper Miocene deposits of the half-graben Porto Torres basin (Funedda *et alii*, 2000). In the western part of the area, the Palaeozoic crystalline basement outcrops, discontinuously covered by the Permian volcano-sedimentary succession. The Mesozoic succession is represented by a sequence of limestone, dolostone and, to a lesser extent, marlstone and evaporitic deposits. The Middle Triassic succession in the Nurra consists mainly of pure dolostone and limestone, with clay-rich beds occurring within the Triassic deposits as marly limestone

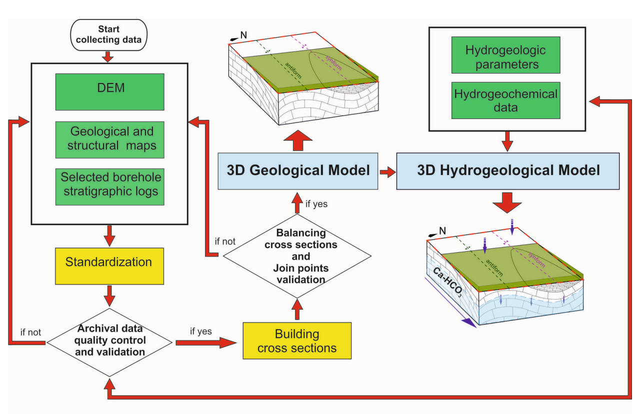

Fig. 1 - Building 3D hydrogeological model methodology

and clayey gypsum deposits. Marls also occur in the Early and Late Jurassic succession. The Jurassic succession mainly consists of limestone and dolostone with a thickness exceeding 700 m. The Lower Cretaceous is represented by pure Urgonian limestone, while the Upper Cretaceous unconformable lies on the Urgonian calcarenite along a bauxite layer, and consists of *Hippurites*-bearing limestone and marl of Late Cretaceous age. The whole Cretaceous sequence has a maximum thickness of about 400 m. The Mesozoic rocks are locally capped by Tertiary pyroclastic rocks and by alluvial sediments of Messinian age, composed mostly of clay and matrix supported conglomerates (Mongelli *et alii*, 2013; Ghiglieri *et alii*, 2009a). The Mesozoic succession is characterized by the superposition of two fold-systems that give to the area a typical dome and basin geometry. The first system affected the Mesozoic carbonate shelf during the Middle Cretaceous and resulted in folds and thrusts trending NW-SE. The second system involved also the Upper Cretaceous and consists of folds trending NE-SW (Oggiano *et alii*, 1987).

Within this geological framework, five main hydrogeological units have been identified, distinguished in turn into seven hydrogeologic complexes, characterized by medium-to-high yield. The main aquifers occur in the Jurassic carbonate sequence and within the carbonate and evaporitic succession of Triassic age (Ghiglieri *et alii*, 2009a; Mongelli *et alii*, 2013).

Geological structures and lithology exert the main control on recharge and groundwater circulation, as well as its availability and quality (Ghiglieri *et alii*, 2009a, b). Groundwater belonging to the Jurassic aquifer shows a dominant calcium-bicarbonate composition with variations to calcium-sulfate/chloride at TDS above 1.1 g/L. The waters from the Triassic aquifer vary from calcium-sulfate to calcium-chloride and finally to sodium-chloride at higher TDS (Ghiglieri *et alii*, 2009a). On the basis of $\delta^{34}S$ and $\delta^{18}O$ values in the dissolved sulfate, the Na-Cl brackish composition of the water hosted by the Jurassic and Triassic aquifers was derived from water–rock interaction processes (Mongelli *et alii*, 2013). The dissolution of evaporitic minerals may also explain the high chloride content, as halite was detected within the gypsum deposits (Mongelli *et alii*, 2013).

MATERIALS AND METHODS

3D hydrogeological model implementation

Surface and subsurface data were employed to reconstruct a 3D geological model. Surface data included geological maps (RAS, 2006b; Mameli *et alii*, 2007; Ghiglieri *et alii*, 2009a; Mongelli *et alii*, 2013; ISPRA, 2014), satellite images, aerial photographs at a scale 1:33,000 and the SAR Digital Elevation Model (10- by 10-m data spacing) generated by the Regional Administration of Sardinia (RAS, http://www.sardegnageoportale.it) using the 3D Analyst and Spatial Analyst extensions of ArcGIS 10.0 (ESRI, Redmond, USA). Subsurface data were essentially derived from borehole stratigraphic logs. Additional data were also collected during considerably field work carried out between 2006 and 2014. In order to build accurate 3D geological models, it was necessary to develop a methodology that takes into account the variety of available data and integrates data that have different descriptive attributes. The flowchart describing the methodology is reported in Fig. 1.

A geodatabase containing all the data (structural, stratigraphic, geochemical, hydrogeological) was developed, to allow easy edit and update the model by integrating new data. The database was designed to address (1) data management, processing and analysis, as well as hydrogeological-conceptual model production; (2) numerical modelling. The geodatabase is largely composed of archival boreholes from different sources, e.g. RAS (110 boreholes logs) and mining companies (168 boreholes logs). Validation procedures and database quality control were carried out according to the criteria and the strategies proposed by Ross *et alii* (2005) and Chesnaux *et alii* (2011) addressed to avoid duplicated data, validate boreholes location and elevation and homogenize geological information. To facilitate correlation between highly detailed descriptions using lithofacies code (e.g., geologic maps) and non-standardized poorly detailed descriptions of the borehole logs, all the data were reclassified integrating the descriptive attributes or the lithofacies code with a standard code as additional attribute. In this way the old descriptions were preserved. The standard code was chosen for hydrogeological purpose; therefore lithologies with the same hydrogeological features were merged and the same standard code was assigned. In this way seven main hydrogeological systems would be identified in the 3D space (Fig. 2).

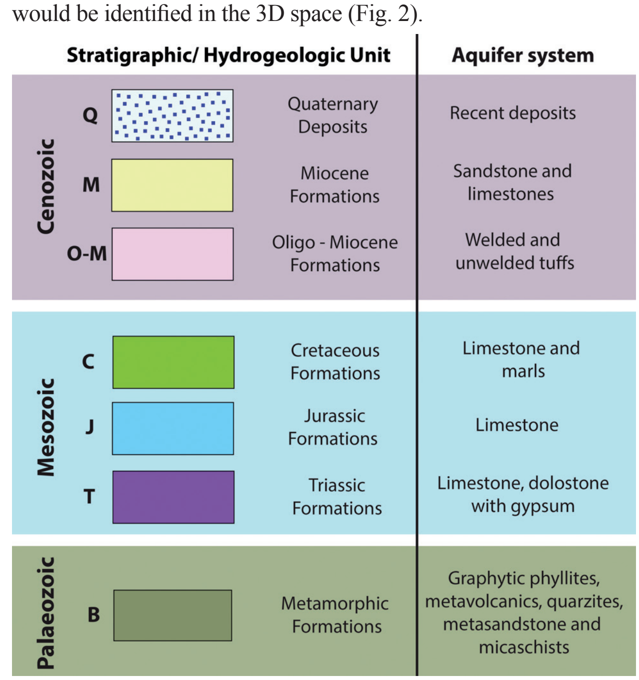

Fig. 2 - Main hydrogeological units identified in the Nurra district and corresponding aquifers

Surface and deep data were digitized and implemented in a GIS using the software ArcGIS 10.0 in order to create and manipulate the data, make spatial analysis and better understand the areal distribution of data.

The 3D modeling has been performed through a stepwise refinement method to make the accuracy of the horizons model to be gradually and effectively improved with data such as DEM, boreholes, cross sections, geological and structural maps. Thus, sixteen geological sections were drawn perpendicular to the main structures (7 oriented SW-NE and 9 oriented NW-SE) by interpreting geological maps and integrating borehole stratigraphic logs (Fig. 3a).

The sections were generated with the ArcGIS eXacto 2.0. The tool generates surface profile (using a DEM), the geologic units and their contact points on the surface, the location of wells/boreholes, and the geologic materials found at the well location, projected as a line into the subsurface. The output was a combination of polyline and point shapefiles. One of the advantages of this software is that the output features have a spatial reference, meaning that, when set to the desired map scale, the cross section measurements will always be correct (Carrel, 2011). The 3D geological model were performed using Midland Valley's 3D MOVE software (www.mve.com/software/move). The software package was used to verify the three dimensional consistency of the geological model. As a first step the geological sections were implemented in the model. Balancing section procedures and join points validation were performed to provide a control of the interpretation and ensure they were geometrically possible and geologically consistent (Fig. 3b). The 3D hydrogeological model has been built according to the conceptual hydrogeological model. Top and down surfaces of each horizon were modelled through the interpolation of horizons depth using the Inverse Distance Weight (IDW) method, honoring the geological cross-sections and the well data (Fig. 4). Flow field and recharge mechanisms of the aquifers were inferred from the hydraulic head contour, based on the observation wells, and hydrogeochemical data.

Sampling and water chemistry data collection

Hydrogeochemical surveys were conducted in September and November 2014. Water samples from 9 springs and 28 wells were collected respectively from the Jurassic limestone and dolostone aquifer (3 springs and 25 wells), from the Miocene detrital sedimentary aquifer (2 springs and 3 wells), and from the Oligo-Miocene volcanic aquifer (4 springs). Groundwater samples were collected mainly from domestic wells, which were consistently pumped. All the samples were filtered in situ through a 0.2 µm pore-size polycarbonate filter with an all-plastic filtration assembly, and acidified upon filtration for metal analyses. At each sampling site, temperature, pH, Eh, alkalinity, dissolved oxygen and conductivity were measured. The Eh was measured by platinum electrode, and the value corrected against the Zobell's solution (Nordstrom, 1977). Alkalinity was determined by acidimetric titration using methyl orange as

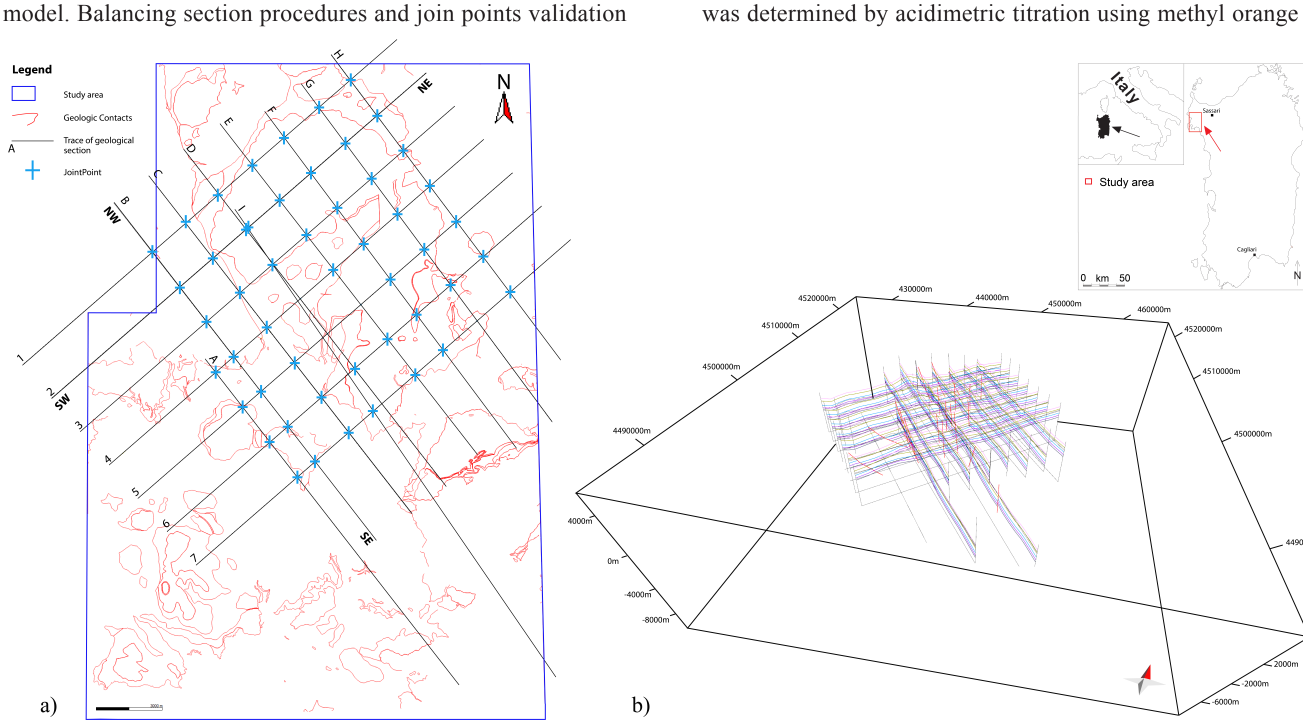

Fig. 3 - a) Trace of geological sections and b) balanced sections built to generate the 3D model

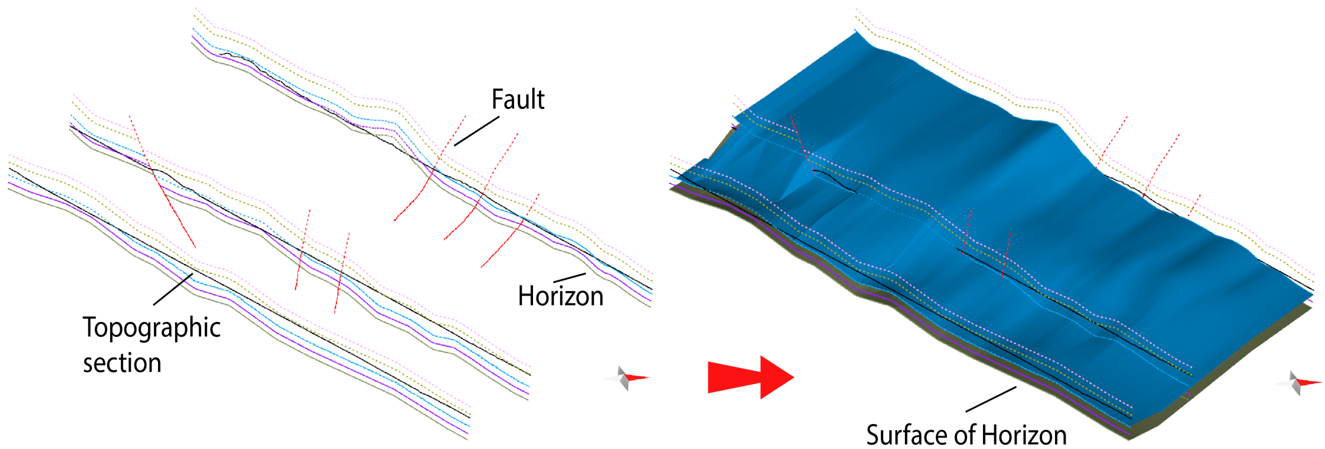

Fig. 4 - Interpolation of horizons from three balanced sections to build geological surfaces

indicator and expressed as bicarbonate ion (HCO_3^-), since CO_3^{2-} was always undetectable and contribution of non-carbonate species negligible. Anions and the nitrogen species (NO_3^-, NO_2^-) were determined by ion chromatography (Dionex ICS3000), and cations by ICP-AES (ARL3520) and ICP-MS (Elan DRC-e). The ionic balance was ≤5%; both precision and accuracy were estimated at 10% or better, using randomly duplicate samples and standard reference solutions (NIST1643e and EnviroMAT™ EP-L-3). Speciation and equilibrium calculations were carried out using the PHREEQC computer program (Parkhurst & Appelo, 1999) and the Lnl database. Saturation index (SI) was calculated as *logIAP/K*, where *IAP* is the product of the activities of the relevant ionic species, and *K* is the solubility product for the specific mineral. Hydrogeochemical dataset reported by Ghiglieri *et alii* (2009a) was also considered in this study.

Statistical analysis and hydrogeochemical mapping

Summary statistics of pH, redox potential (Eh), electrical conductivity (EC), major ions, nitrates and bromide for the groundwater of the Nurra region included the calculation of minimum, maximum, mean, median, standard deviation, 75th and 25th percentile values and variance. To describe the statistic distribution, skewness and kurtosis were also provided.

Principal Component Analysis (PCA) were carried out to reveal hidden pattern in the dataset and to distinguish groundwater family patterns. PCA reduces the complexity of multivariate datasets transforming the original input variables into a lower dimension dataset. It involves a calculation of a covariance matrix of a dataset to minimize the redundancy and maximize the variance in order to define the principal components of input data. The principal components are uncorrelated variables that have the greatest variance. They are plotted as orthogonal axis in the so called covariance biplot or correlation biplot. In the PCA biplot the samples are represented as points, while the variables are represented as labelled, calibrated axes. The covariance biplot adjusts the points and axes of the PCA biplot so that the cosines of the angles between the axes approximate the correlations between the corresponding variables. The correlation biplot is similar, except that the variables are first scaled to have unit variances (La Grange, 2009). In PCA biplots all the hydrogeochemical information of a sample are integrated into a single number allowing the simultaneous analysis of those parameters that control the variability of the data (Raiber *et alii*, 2012). For the PCA both geochemical data produced for this study and the dataset reported by Ghiglieri *et alii* (2009a) were considered all together. Various geochemical mapping techniques were used for presenting and interpreting the data. Distribution data pattern were recognized using proportionally sized dots map.

RESULTS

3D hydrogeological model

The 3D geological model was based on stratigraphic logs and validated by balanced geological cross sections oriented NE-SW and NW-SE, respectively parallel and perpendicular to the main structures. It produced a consistent representation of geological structures geometry for modelling hydrogeological features. Two main fold systems were recognized. The oldest one is made up by Middle Cretaceous open upright folds with axes NW-trending and dipping to SE, wave length of about 1 km and amplitude about 100 m. The youngest consists of NE-trending folds, affecting the Upper Cretaceous formation, that are responsible for the change of the axes plunge of NW-trending folds. The interference between the two fold systems highly influenced the flow field of aquifers, producing drainage axes dipping mainly towards NE in the northern sector of the study area and towards SW in the southern sector. NW-striking, low-angle thrusts, related to the NW-trending folds, placed

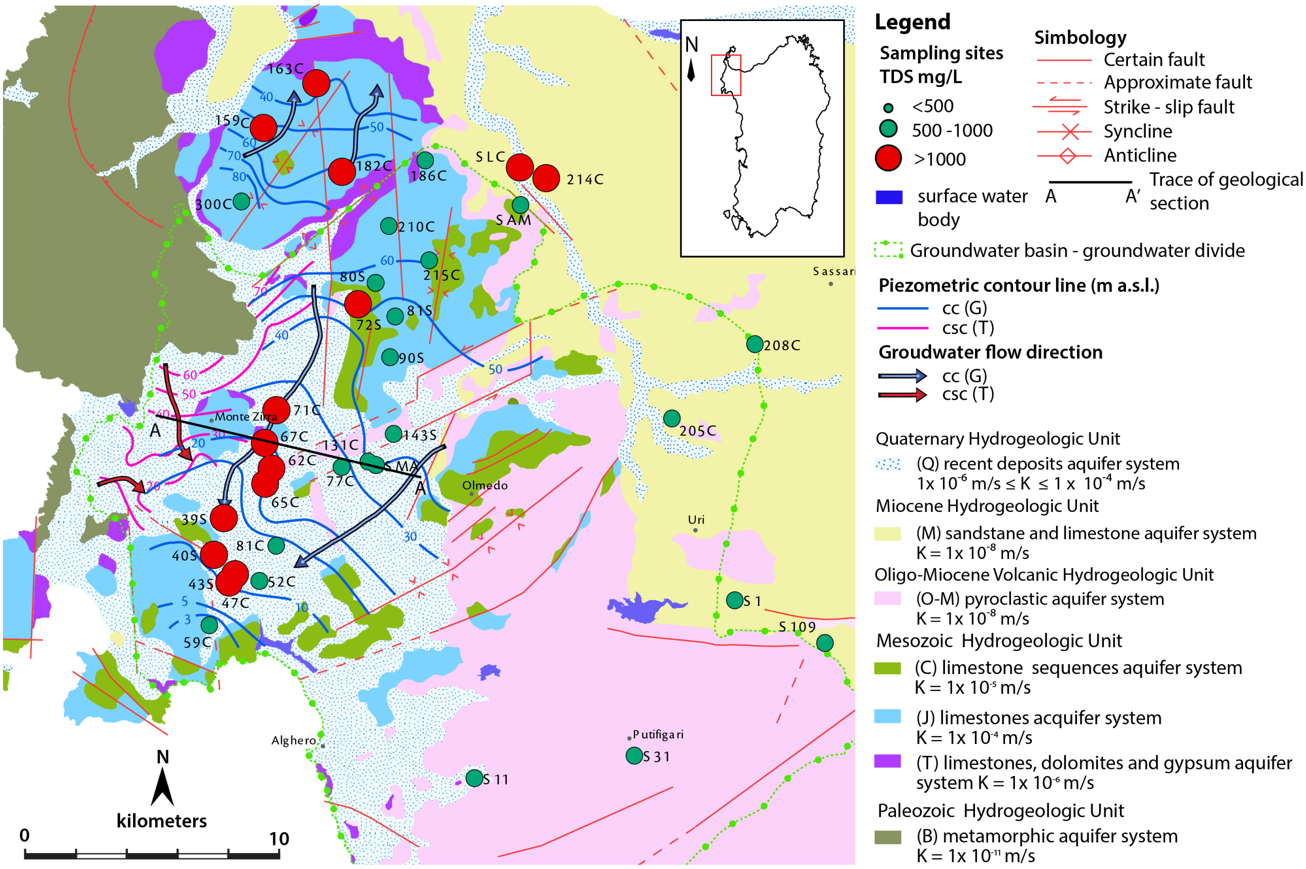

Fig. 5 - Hydrogeological map of the Nurra district (from Ghiglieri et alii, 2009a, modified); concentration of Total Dissolved Solids is shown as proportional dots at each sampling site

laterally in contact the Jurassic and Triassic aquifers (Fig. 5). As a consequence, according to the hydraulic head contour line and groundwater flow directions reported by Ghiglieri *et alii* (2009a), an indirect recharge of the Jurassic aquifer through the Triassic one would occur (Fig. 5 and Fig. 6).

Water chemistry and statistical analysis

According to stratigraphic well log, groundwater samples were classified into three groups on the basis of the hosting aquifer (M - Miocene sandstone and limestone, OM – Oligo-Miocene volcanic rocks, J - Jurassic limestone and dolostone). Table 1 reports summary statistics of main hydrogeochemical parameters of groundwater sampled during the 2014 surveys, grouped according to the hosting aquifer. Groundwaters show near neutral or slightly alkaline pH (6.4-7.75) and the conductivity (EC) values range between 700 µS/cm and 1800 µS/cm. The lower EC values were measured on OM wells which also have lower nitrate compared to other groups. The redox potential values indicated oxidizing conditions (Eh=0.3 to 0.5 V) for all groundwaters. Jurassic groundwater shows the higher median concentrations of Ca, HCO_3 and SO_4, whereas OM wells have high median concentration of Na and Cl compared to the other groundwater groups. The highest concentration of nitrate was measured in Jurassic and Miocene groundwater.

Multivariate statistical analysis was performed through the Principal Component Analysis to distinguish groundwater family patterns. Data were log transformed, centered and scaled. Taking into account components with Eigenvalue greater than 1, three principal components (PCs) were identified for the Nurra groundwater. All three PCs account for more than 77% of the variability in the original data set. Table 2 reports the relative contribution of any original variable to each PC. PC1 shows a negative loading of NO_3 and a strong positive weightings of EC, Mg, K, Na, Cl and SO_4. Silica and Br have minimal influence on the PC1, being these variables close to the zero line. This PC1 may indicate the distinction between more evolved waters with high EC and high concentrations of dissolved ions and less evolved groundwater with lower EC. Nitrate is inversely related to EC and all dissolved ions, thus it can be stated that the sources of nitrate are different from those of the other variables.

PC2 shows a strong positive loadings of Ca and HCO_3 and a

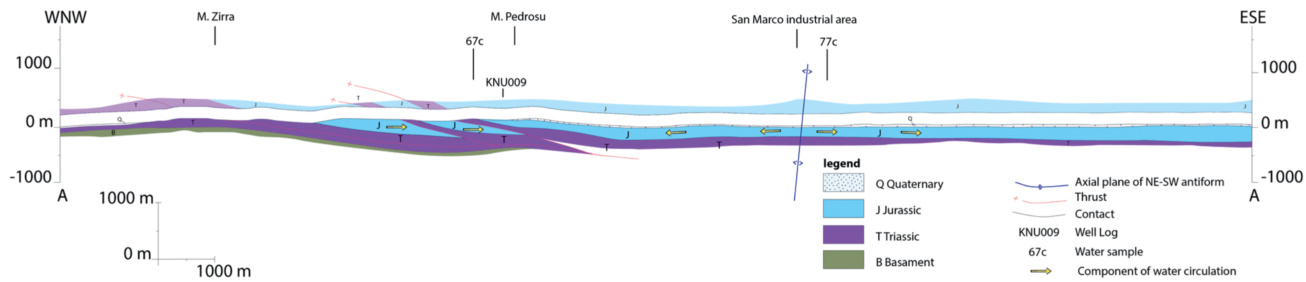

Fig. 6 - Geological cross section WNW-ESE showing the connection between Jurassic and Triassic aquifers. The trace of the section is reported in Fig. 5 (A-A')

	T °C	pH	Eh mV	EC mS/cm	TDS mg/L	Ca mg/L	Mg mg/L	K mg/L	Na mg/L	HCO_3 mg/L	Cl mg/L	SO_4 mg/L	NO_3 mg/L	SiO_2 mg/L	Br mg/L
Miocene Hydrogeologic Unit (M)															
N	5	5	5	5	5	5	5	5	5	5	5	5	5	5	4
Min	16.5	6.95	353	0.80	608	52	5.6	1.3	41	328	74	18	16	8	0.3
Max	20.2	7.33	442	1.80	1104	173	26	11	157	412	290	61	70	17	0.7
Mean	18.9	7.12	409	1.12	783	108	12	4.4	86	367	143	33	28	12	0.5
Median	19.8	7.06	405	0.90	691	104	7.4	2.2	61	359	90	24	19	11	0.5
SD	1.6	0.17	36	0.42	213	43	8.6	4.1	51	38	94	18	23	3	0.2
25^{th}	17.2	6.97	378	0.84	613	75	6.0	1.6	45	332	75	20	16	9	0.3
75^{th}	20.2	7.31	442	1.53	999	143	21	8.2	140	406	238	50	45	145	0.7
Variance	3	0.03	1330	0.17	45450	1870	74	17	2610	1420	8890	305	538	11	0
Skewness	-1.0	0.4	-0.9	1.5	1.0	0.5	1.2	1.6	0.7	0.3	1.2	1.3	2.2	1.0	0.0
Kurtosis	-1.1	-2.9	0.4	1.5	-0.4	1.9	0.1	2.1	-2.0	-2.7	0.2	0.9	4.8	0.2	-5.7
Oligo-MiceneVolcanic Hydrogeologic Unit (OM)															
N	4	4	4	4	4	4	4	4	4	4	4	4	4	4	4
Min	15.4	6.45	413	0.70	390	21	16	4.7	76	87	140	21	2.8	35	0.5
Max	23.7	6.91	460	1.62	880	48	29	13	200	123	413	50	9	76	1.7
Mean	18.9	6.77	440	1.14	619	31	22	7	140	106	271	36	6	52	1.0
Median	18.3	6.87	443	1.12	602	28	21	5	142	106	265	36	6	48	1
SD	3.6	0.22	21	0.38	204	12	6	4	53	15	113	13	3	17	0.5
25^{th}	15.9	6.55	418	0.79	432	23	17	5	88	92	167	23	3	38	0.6
75^{th}	22.6	6.91	458	1.51	822	43	27	11	189	119	380	48	9	69	1.5
Variance	13	0.05	449	0.14	41670	132	30	17	2760	211	12680	156	8	303	0
Skewness	0.9	-1.9	-0.6	0.3	0.5	1.6	0.7	2.0	-0.2	-0.2	0.3	-0.2	0.1	1.2	0.6
Kurtosis	0.6	3.6	-1.7	1.0	0.7	3.0	1.1	3.9	-0.4	1.2	1.2	-0.8	-3.7	2.2	1.2
Jurassic limestone and dolostone aquifer (J)															
N	28	28	28	28	28	28	28	28	28	28	28	28	28	28	25
Min	16	6.77	324	0.94	747	103	10	1.2	57	305	78	19	6	6	0.01
Max	22	7.75	480	1.80	1293	185	41	18	181	575	318	118	67	19	1.2
Mean	19	7.03	422	1.33	1010	140	25	5	107	466	175	72	20	10	0.5
Median	19	6.99	423	1.27	936	135	24	5	101	467	146	68	17	9	0.4
SD	1	0.21	32	0.29	173	23	7	3	39	58	83	27	14	3	0.3
25^{th}	18	6.89	411	1.07	849	120	20	3	71	430	104	48	13	9	0.3
75^{th}	19	7.12	443	1.66	1163	155	30	6	147	497	249	94	22	11	0.7
Variance	1	0.04	1010	0.08	29820	544	54	11	1540	3410	6930	730	185	8	0
Skewness	0.0	1.7	-0.9	0.3	0.2	0.5	0.0	2.7	0.5	-0.3	0.6	-0.1	2.6	1.8	0.7
Kurtosis	1.4	3.9	2.3	-1.5	-1.5	-0.8	0.1	9.5	-1.2	1.2	-1.2	-0.9	7.1	3.6	0.3

SD=Standard deviation; 25^{th} and 75^{th} = 25 percentile and 75 percentile

Tab. 1 - Summary statistics for samples collected in the Nurra district grouped according to different hosting aquifer (M, O-M, and J samples)

Variable		Principal component	
	PC1	PC2	PC3
Log10 (EC)	0.44	0.06	-0.04
Log10 (Ca)	0.18	0.53	0.16
Log10 (Mg)	0.40	0.05	0.15
Log10 (K)	0.37	-0.21	-0.08
Log10 (Na)	0.42	-0.15	-0.07
Log10 (SiO_2)	-0.01	-0.44	0.55
Log10 (HCO_3)	0.06	0.55	-0.27
Log10 (Cl)	0.42	-0.15	0.00
Log10 (SO_4)	0.29	0.22	0.39
Log10 (NO_3)	-0.18	0.22	0.54
Log10 (Br)	0.01	-0.20	-0.35
Percentage of explained variance	0.44	0.22	0.22
Cumulative proportion (%) of variance	0.44	0.67	0.67
Eigenvalue	4.80	2.48	2.48

Tab. 2 - Table of component loadings, explanation of variance percentage and cumulative (%) and Eigenvalue for the PCs identified

negative weightings of SiO_2, Na, Cl, K and Br. The PC2 may be representative of Ca-HCO_3 type waters. They are quite distinct from Na-Cl type, as Na and Cl show the opposite behavior.

PC3 may be representative of water-silicate minerals interaction. Indeed PC3 results show a very strong loading of SiO_2.

DISCUSSION

Hydrogeochemical investigation showed that no actual variations of the main hydrogeochemical features occurred with respect to those reported by Ghiglieri *et alii* (2009a). TDS of waters ranges between 0.4 and 1.3 g/L and springs generally showed lower salinity than wells. Groundwater from Jurassic aquifer showed a TDS values ranging from 0.7 to 1.3 g/L and a median value higher than that observed in groundwater from Miocene sedimentary and Oligo-Miocene volcanic aquifers. Mapping the salinity according to the proportionally sized dots method (Fig. 5), it can be observed that higher salinity affects mainly groundwater occurring in the western and in the northern sectors of the Jurassic hydrogeologic unit, whereas in the eastern-sector of the Jurassic aquifer waters show TDS lower than 1.0 g/L.

Spatial distribution of salinity and geochemical features of groundwater samples reflected the type of rocks with which the waters were interacting. Indeed the western-Jurassic groundwater exhibited a more chloride character as compared to the dominant bicarbonate in the eastern groundwater. Figure 7a shows the Piper Diagram of the sampled waters. Jurassic groundwater were distinguished in J(W) and J(E) in order to recognize different water type within the aquifer. The composition area were Triassic waters fall in is also reported (data from Ghiglieri *et alii,* 2009a). Jurassic western groundwater evolved to approximate the composition of groundwater hosted in the Triassic formations. Moreover, calcium-sulfate molar ratio in Jurassic groundwater decreases as chloride content increases, approximating values observed in Triassic groundwater (Fig. 7b). As indicated by saturation index (SI) calculation, the increasing concentration of sulfate in groundwater is conjugated with an approach to equilibrium with respect to gypsum. These observations suggest

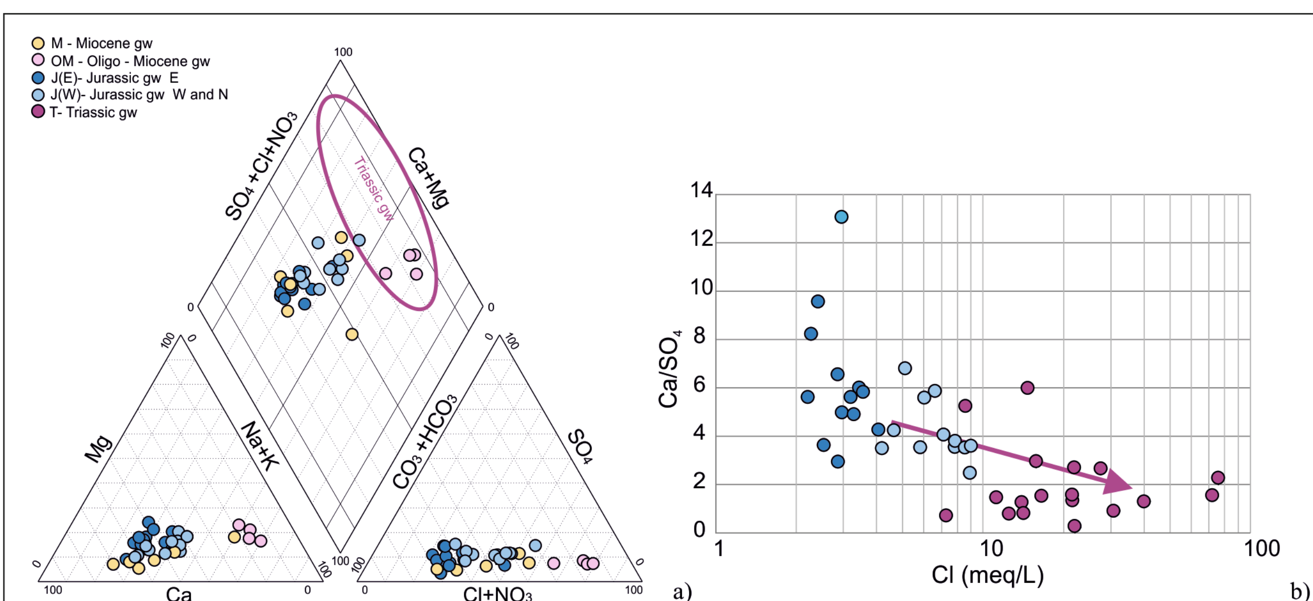

Fig. 7 - a) Piper Diagram for the groundwater of the Nurra region and b) Ca/SO_4 vs Cl plot for the Jurassic and Triassic groundwater. Triassic groundwater data derived from Ghiglieri et alii (2009a)

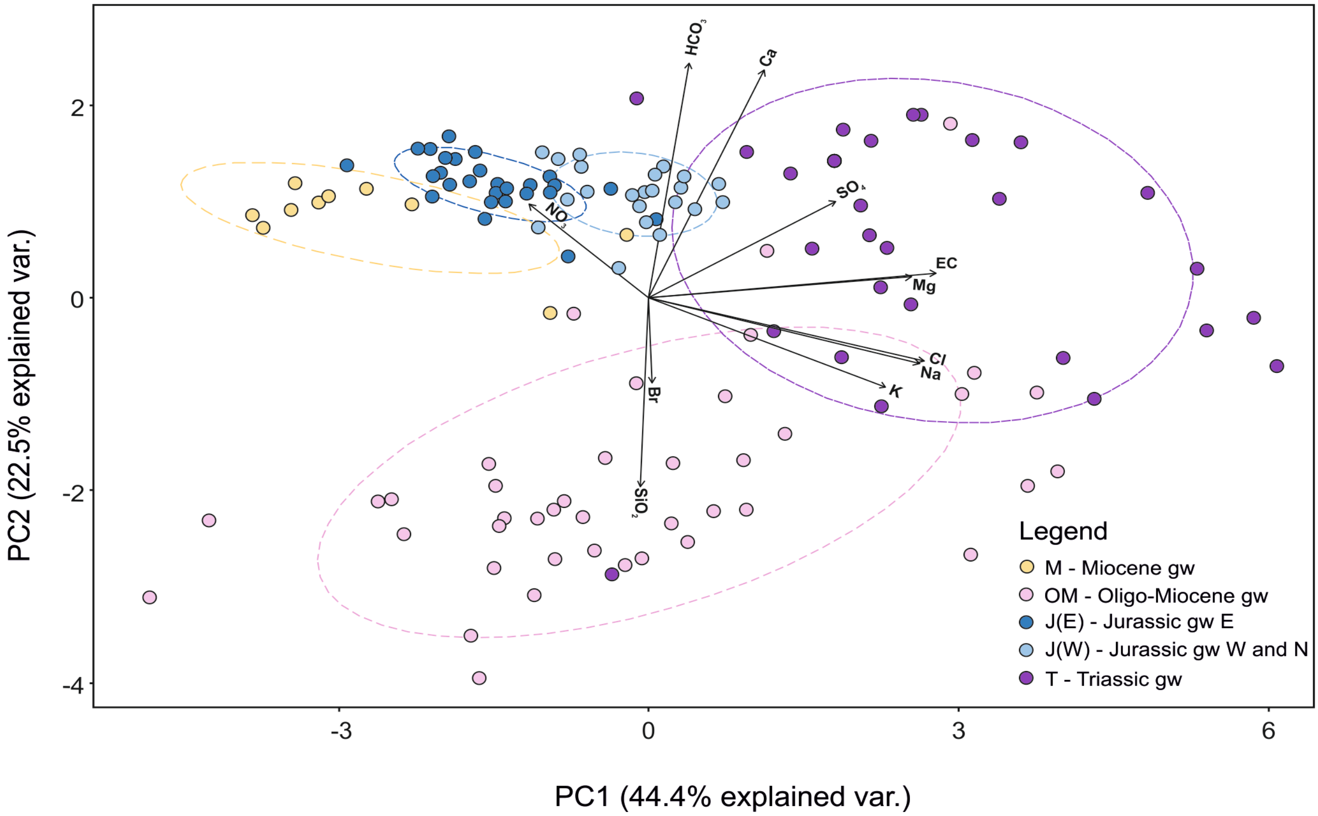

Fig. 8 - Correlation biplot of variable weights in PC1 and PC2 identified by PCA for the groundwater of the Nurra region. Data of Triassic groundwater are from G*higlieri et alii (2009a)*

an interaction of water with the Triassic-evaporites, according to the hydrogeological model proposed. PCA correlation biplot (Fig. 8) points out that Jurassic western samples (J(W)) have an intermediate behavior between the Triassic groundwater and the Jurassic eastern wells.

These results confirmed that the Triassic and Jurassic aquifers are locally connected. Trends of piezometric head and groundwater flow directions also supported this statement (Fig. 5 and Fig. 6). Such finding will be further investigated performing $\delta^{34}S$ and $\delta^{18}O$ isotopes analyses and implementing them in the developed 3D hydrogeological model.

CONCLUSIONS

A hydrogeological 3D modelling supported by hydro-geochemical mapping and the integrated interpretation of data were performed. This innovative approach, applied to the case study of the Nurra region, highlighted that structural history of the Nurra region exerts a considerable control on hydrogeology and hydrochemistry of groundwater. The applied methodology provided further information about the relationship between lithology and groundwater geochemistry and enabled us to reach new findings regarding the boundary conditions of the strategic aquifers. These findings could help calibrate a coupled numerical groundwater flow and solute transport model of the Nurra area. While highly useful for groundwater management, such models are notoriously difficult to constrain, and applying geochemical and isotope data as calibration targets is a promising and evolving area of research. The methodology presented in this paper demonstrated that the combination of geochemical mapping and 3D hydrogeological modelling, integrated with multivariate statistical analysis, resulted a powerful tool for carrying out the hydrogeological reconstruction of a complex area. The resulted knowledge-base system is needful for understanding and monitoring transfer dynamics of pollutants into groundwater and can serve the government authorities to better manage water resources in many complex hydrogeological situations.

ACKNOWLEDGMENTS

This research was conducted in the frame of the KNOW project (Coordinator R. Cidu) funded by the Autonomous Region of Sardinia (Italy) 2012–14, under the Regional Law 7/2007: "Promotion of scientific and technological innovation in Sardinia". Authors acknowledge the advice of Prof. Giacomo Oggiano regarding fundamental geology.

REFERENCES

ARPA Sardegna (2009) - *Progetto pilota di lotta alla desertificazione nelle cinque regioni italiane maggiormente a rischio: Regione Sardegna. Relazione conclusiva.* 164 pp. http://www.minambiente.it/sites/default/files/archivio/allegati/desertificazione/Sardegna.pdf

Carrel J. (2011) - *Tools and techniques for 3D geologic mapping in ArcScene: boreholes, cross sections, and block diagrams.* Digital Mapping Techniques '11–12-Workshop Proceedings. U.S. Geological Survey Open-File Report 2014–1167. http://pubs.usgs.gov/of/2014/1167/

Chesnaux R., Lambert M., Walter J., Fillastre U., Hay M.. Rouleau A., Daigneault R., Moisan A. & Germaneau D. (2011) - *Building a geodatabase for mapping hydrogeological features and 3D modeling of groundwater systems: Application to the Saguenay–Lac-St.-Jean region. Canada.* Computers & Geosciences, **37**: 1870-1882.

Da Pelo S., Ghiglieri G., Buttau C., Cuzzocrea C., Carletti A., Biddau R., Fenza P., Arras C., Funedda A. & Cidu R. (2015) - *3D hydrogeological modelling supported by geochemical mapping as an innovative approach for management of aquifers applied to the Nurra district (Sardinia, Italy).* Rendiconti Online Societa Geologica Italiana, **35**: 300-303. Doi: 10.3301/ROL.2015.125

Funedda A., Oggiano G. & Pasci S. (2000) - *The Logudoro basin: a key area for the Tertiary tectono-sedimentary evolution of North Sardinia.* Boll. Soc. Geol. It., **119**: 31-38.

Ghiglieri G., Oggiano G., Fidelibus D., Barbieri G., Vernier A. & Tamiru A. (2009a) - *Hydrogeology of the Nurra Region, Sardinia (Italy): basement-cover influences on groundwater occurrence and hydrogeochemistry.* Hydrogeol. J, **17** (2): 447-466.

Ghiglieri G., Barbieri G., Vernier A., Carletti A., Demurtas N., Pinna R. & Pittalis D. (2009b) - P*otential risks of nitrate pollution in aquifers from agricultural practices in the Nurra region, northwestern Sardinia, Italy.* J. Hydrol, **379**: 339-350. Doi: 10.1016/j.jhydrol.2009.10.020.

Ghiglieri G., Carletti A. & Pittalis D. (2012) - *Analysis of salinization in the coastal carbonate aquifer of Porto Torres (NW Sardinia, Italy).* J. Hydrol., **432-433**: 43-51. Doi:10.1016/j.jhydrol.2012.02.016.

Ghiglieri G., Carletti A. & Pittalis D.(2014) - *Runoff coefficient and average yearly natural aquifer recharge assessment by physiography-based indirect methods for the island of Sardinia (Italy) and its NW area (Nurra).* Journal of Hydrology, **519**: 1779-1791. Doi: 10.1016/j.jhydrol.2014.09.054

Ghiglieri G., Carletti A., Da Pelo S., Cocco F., Funedda A., Loi A., Manta F. & Pittalis D. (2016) - *Three-dimensional hydrogeological reconstruction based on geological depositional model: a case study from the coastal plain of Arborea (Sardinia, Italy).* Engineering Geology, **207**: 103-114. Doi:10.1016/j.enggeo.2016.04.014

ISPRA - Servizio Geologico d'Italia (2014) - *Carta Geologica d'Italia alla scala 1:50.000. Foglio 459. Sassari.* Progetto CARG. http://www.isprambiente.gov.it/Media/carg/459_ SASSARI/Foglio.html

La Grange A.M., Le Roux N.J. & Gardner-Lubbe S. (2009) - *BiplotGUI: Interactive Biplots in R*. Journal of Statistical Software, **30**: 12, 1-37. http://www.jstatsoft.org/v30/i12.

Lancianese V. & Dinelli E. (2015) - *Different spatial methods in regional geochemical mapping at high density sampling: An application on stream sediment of Romagna Apennines. Northern Italy.* Journal of Geochemical Exploration, **154**: 143-155. Doi:10.1016/j.gexplo.2014.12.014.

Mameli P., Mongelli G., Oggiano G. & Dinelli E. (2007) - *Geological, geochemical and mineralogical features of some bauxite deposits from Nurra (Western Sardinia. Italy): insights on conditions of formation and parental affinity*. Int. J. Earth Sci. (Geol Rundsch), **96**: 887-902. Doi: 10.1007/s00531-006-0142-2.

Mongelli G., Monni S., Oggiano G., Paternoster M. & Sinisi R. (2013) - *Tracing groundwater salinization processes in coastal aquifers: a hydrogeochemical and isotopic approach in the Na-Cl brackish waters of northwestern Sardinia. Italy.* Hydrol. Earth Syst. Sci., **17**: 2917-2928. Doi:10.5194 /hess-17-2917-2013.

Nordstrom D.K. (1977) - *Thermochemical redox equilibria of Zobell's solution.* Geochimica et Cosmochimica Acta, **41**: 1835-1841.

Ohta A., Imai N., Terashima S. & Tachibana Y. (2015) - *The spatial distribution of multiple elements in the Kanto region of Japan: Transport of chalcophile elements from land to sea.* Journal of Geochemical Exploration. **154**: 156-170. Doi: 10.1016/j.gexplo.2014.11.016.

Oggiano G., Sanna G. & Temussi I. (1987) - *Caractéres géologiques et géochemiques de la bauxite de la region de la Nurra.* Groupe Français du Crétacé. Sardinia 24-29 Mai 1987, 72-124.

Parkhurst D.L. & Appelo C.A.J. (1999) - *User's guide to PHREEQC (version 2) - A computer program for speciation, batch-reaction, one-dimensional transport, and inverse geochemical calculations.* USGS Water-Resources Investigations Report 99–4259, Denver, Colorado.

Raiber M., White P.A., Daughney C.J., Tschritter C., Davidson P. & Bainbridge S.E. (2012) - *Three-dimensional geological modelling and multivariate statistical analysis of water chemistry data to analyse and visualise aquifer structure and groundwater composition in the Wairau Plain. Marlborough District. New Zealand.* Journal of Hydrology, **436-437**: 13-34. Doi:10.1016/j.jhydrol.2012.01.045.

RAS - Regione Autonoma della Sardegna (2006a) - *Piano regolatore generale degli acquedotti della Sardegna - All. 2/b - Previsione della popolazione residente e fluttuante stagionale. Vol. I - Comuni del Sassarese.* http://www. regione.sardegna.it/documenti/1_5_20060727123714.pdf

RAS - Regione Autonoma della Sardegna (2006b) - *Carta Geologica della Sardegna. Sardegna Mappe carte tematiche.* http://www.sardegnageoportale.it/webgis2/sarde gnamappe/?map=mappetematiche

RAS - Regione Autonoma della Sardegna (2014) - *Progetto di Aggiornamento del Piano di Gestione del Distretto Idrografico - Caratterizzazione. obiettivi e monitoraggio dei corpi idrici sotterranei.* Allegato Delibera Comitato Istituzionale n. 4 del 18.12.2014. http://www.regione.sarde gna.it/documenti/1_470_20141222141305.pdf

Ross M., Parent M. & Lefebvre R. (2005) - *3D geologic framework models for regional hydrogeology and land-use management: a case study from a Quaternary basin of southwestern Quebec. Canada.* Hydrogeology Journal, **13**: 690.707. Doi: 10.1007/s10040-004-0365-x.

Wu Q., Xu H. & Zou X. (2005) - *An effective method for 3D geological modeling with multi-source data integration.* Computers & Geosciences, **31**: 35-43. doi:10.1016/j.cageo.2004.09.005.

Zhu L., Zhang C., Li M., Pan X. & Sun J. (2012) - *Building 3D solid models of sedimentary stratigraphic systems from borehole data: an automatic method and case studies.* Engineering Geology, **127**: 1-13. Doi:10.1016/j.enggeo. 2011.12.001

Received January 2016 - Accepted May 2016